

# Ablation behaviour of a TaC coating on SiC coated C/C composites at different temperatures

Yong-jie Wang, He-jun Li\*, Qian-gang Fu, Heng Wu, Lei Liu, Can Sun

*State Key Laboratory of Solidification Processing, Northwestern Polytechnical University, Xi'an 710072, PR China*

Received 7 May 2012; received in revised form 6 June 2012; accepted 11 June 2012

Available online 17 June 2012

## Abstract

To improve the ablation resistance of carbon/carbon (C/C) composites, a TaC coating was prepared by supersonic plasma spraying on SiC coated C/C composites. The microstructure and morphology of the coatings were characterised by Scanning Electron Microscopy and X-ray diffraction. The ablation properties were studied at different temperatures under oxyacetylene torch. At 2100 °C, the oxides were blown away and resulted in high ablation rates:  $1.2 \times 10^{-2}$  mm/s and  $3.9 \times 10^{-3}$  g/s. However, most oxides can remain in ablation centre and serve as a coating at low temperature (1900 and 1800 °C). Therefore, the TaC/SiC coated samples exhibited zero linear ablation rate and lower mass ablation rate.

© 2012 Elsevier Ltd and Techna Group S.r.l. All rights reserved.

**Keywords:** B. Composites; C. Corrosion; E. Thermal applications

## 1. Introduction

Carbon/carbon composites (C/C) are appropriate structural materials in ultra-high-temperature environments due to their outstanding thermal properties [1–3]. However, without protection these composites will be damaged by ablation at high temperature above 2000 °C [4]. In order to improve the ablation resistance of C/C composites and ensure the composites have a longer service life, refractory carbides have been introduced into C/C composites [5]. TaC has always been concerned because it has some remarkable properties such as high hardness, high melting point (above 3880 °C) and good thermal conductivity [6,7]. Up to now, two ways are commonly used to improve ablation resistance of C/C composites by TaC. One way is to add TaC into the matrix of these composites. Xiang et al. [8] prepared Tantalum carbide materials in C/C composites by liquid precursor conversion method. The TaC grain size enlarged with temperature elevating. Wang et al. [9] introduced TaC powders into C/SiC composites using slurry infiltration method. The glass state Ta<sub>2</sub>O<sub>5</sub> can

improve anti-ablation performance at ultra-high temperature. Chen et al. [10] fabricated C/C composites with SiC–TaC inter layer through isothermal chemical vapour infiltration. But, the tantalum compounds were not able to seal off the material surface during ablation. A uniform, adherent and crack-free TaC coating was obtained on carbon fibres using a molten salt method by Dong et al. [11], and thermo-gravimetric analysis indicated that the oxidation resistance of carbon fibre can be improved remarkably with a high-quality TaC layer. In these methods, TaC served as additives in matrix to abate ablation of C/C composites. However, TaC phase cannot be homogeneously introduced, which has a negative effect on the mechanical properties of the composites. Furthermore, it is limited to improve the ablation resistance of C/C composites and the modified composites still show high ablation rates, through these methods.

The other way is to prepare TaC coating on the surface of C/C composites. TaC coating was fabricated on C/C surface using ethylate tantalum as precursor by He et al. [12], the coating had single phase composition after treatment above 1400 °C. But, the coating seemed loosen and large amounts of defects (cracks, pinholes) existed in the coating, which are disadvantageous for the ablation

\*Corresponding author. Tel.: +86 29 88495004; fax: +86 29 88492642.

E-mail address: [lihejun@nwpu.edu.cn](mailto:lihejun@nwpu.edu.cn) (H.-j. Li).

resistance. Li et al. [13], Chen et al. [14] have prepared TaC coating by means of chemical vapour deposition (CVD) and developed several TaC coating systems on C/C surface. These coatings have dense surface, and performed better ablation properties. But, the CVD is an expensive method. Moreover, the controlling of TaCl<sub>5</sub> sublimation process needs high requirements of the equipment. Low temperature phase of Ta<sub>2</sub>C is always accompanied in the TaC coating, which has adverse effects on the ablation resistance.

In this work, supersonic plasma spraying was employed to prepare a TaC coating on SiC coated C/C composites. It is a simple and low-cost way. Compared with traditional plasma spraying, the plasma temperature is above 10000 °C and it has a jet velocity up to 600 m/s [15,16]. Dense coating with better bond can be obtained by this method. The phase compositions and microstructures of the as-prepared coating were discussed. Meanwhile, the coating ablation test was carried out at different temperatures, in order to study the oxides state during ablation.

## 2. Experimental

### 2.1. Preparation of TaC/SiC coated C/C composites

The substrates ( $\Phi$  30 mm  $\times$  10 mm) were cut from bulk 2-D C/C composites. The composites were fabricated through isothermal chemical vapour infiltration with a final density of 1.78 g/cm<sup>3</sup>. Then, the specimens were hand-abraded using 300 grit SiC paper, cleaned with distilled water and dried at 200 °C for 2 h.

The as-received samples were embedded in mixed powder in a graphite crucible, of which the composition is 65 wt% Si, 20 wt% graphite and 15 wt% Al<sub>2</sub>O<sub>3</sub>. The crucible was placed into furnace and held at 2000–2200 °C for 2 h to obtain a SiC coating. Details have been reported in Ref. [17].

Then TaC coating was prepared on SiC coated composites through supersonic plasma spraying. TaC powder (purity > 99.9%) was provided by ZhuZhou GuangYuan Cemented Material Co., Ltd. The size of TaC grains was 1–1.5  $\mu$ m. The argon was employed as the primary gas and the carrier gas. The hydrogen was used as the secondary gas. Details of the spraying parameters are listed in Table 1. The details of the spraying have been described in Ref. [15].

Table 1  
The spraying parameters for the TaC coating.

Spraying voltage (V)	360–400
Spraying current (A)	140–170
Spraying distance (mm)	90
Primary gas (Ar) flow rate (L/min)	80–100
Secondary gas (H <sub>2</sub> ) flow rate (L/min)	30–40
Carrier gas (Ar) flow rate (L/min)	6–10
Powder feeding rate (g/min)	about 35
Nozzle diameter (mm)	4.5

### 2.2. Ablation tests and microstructure analysis

Ablation behaviour was tested under oxyacetylene torch. The TaC/SiC-coated samples were placed vertically to the flame. The inner diameter of the nozzle tip of the ablation gun was 2.5 mm. The surface temperature was detected through optical pyrometer. In our work, three different ablation temperatures were employed in the ablation (2100, 1900 and 1800 °C). The temperatures were chosen around the melting point of Ta<sub>2</sub>O<sub>5</sub> (1872 °C), in order to analyse the fusant state after ablation. The linear and mass ablation rates of the samples could be obtained according to Eqs. (1) and (2) below.

$$R_l = \Delta d / t \quad (1)$$

$$R_m = \Delta m / t \quad (2)$$

$R_l$  is linear ablation rate;  $\Delta d$  is the change of the sample's thickness at centre region before and after ablation;  $R_m$  is mass ablation rate;  $\Delta m$  is sample's mass change before and after ablation;  $t$  is ablation time.

The ablation morphology, microstructure and elemental composition of TaC/SiC coated composites were examined by scanning electron microscope (FE-SEM SUPRA-550). The phases of the coating were characterised by Rigaku D/max-3C X-ray diffraction (XRD, 40 kV, 35 mA, Cu K $\alpha$ ).

## 3. Results and discussion

### 3.1. Microstructures of the coating

From Fig. 1, it can be seen that the coating is composed of TaC and Ta<sub>2</sub>O<sub>5</sub>. During spraying, the plasma could offer high temperature above 10,000 °C, and the TaC powder would be quickly melted under the plasma torch. However, the melted TaC can be oxidised into Ta<sub>2</sub>O<sub>5</sub> according to Eqs. (3) and (4). Therefore, Ta<sub>2</sub>O<sub>5</sub> phases are detected in the XRD pattern.

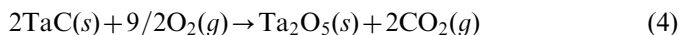
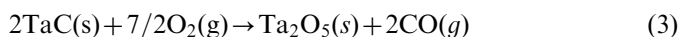


Fig. 2 is the surface and cross section BSE images of the TaC/SiC coating. The coating is covered by lots of white mottles, and no cracks are found on the surface (Fig. 2a). From the magnified image (Fig. 2b), the white mottles can be recognised as fusing state, from which the formation mechanism of the coating can be inferred. During ablation, the TaC was fused in a short time. The melted grains crashed and spread out on the surface of substrate, formed the TaC layer. This process was repeated and finally a thick coating was obtained. In spraying, gases (such as air, CO or CO<sub>2</sub>) may be mingled into the powder, so small pinholes can be observed at the surface. Owing to the high speed of the plasma flame, the oxidation of TaC and the mingled gases were much less than that of the normal speed spraying. That is the reason why supersonic plasma spraying can get a dense coating (Fig. 2c). The SiC and

TaC coatings can be distinguished easily, with thickness of about 50 and 250  $\mu\text{m}$  respectively.

### 3.2. The ablation behaviour of the TaC/SiC coating

From Fig. 3a, it can be found that the surface temperature rises quickly in the first 30 s for the 2# and 3# curves. After 30 s the temperature increases very slowly and finally stays almost at a fixed value, which is close to our test temperature. It is because that a heat balance may be achieved between the heating (from oxyacetylene flame) and cooling processes (heat emission and transmission

from water cycling system). Thus, the surface temperature will stop to rise. Meanwhile, the evaporation of  $\text{Ta}_2\text{O}_5$  consumed a large amount of heat, which could lower the surface temperature. As to the three temperatures, 2100  $^{\circ}\text{C}$  and 1900  $^{\circ}\text{C}$  are above the melting point of  $\text{Ta}_2\text{O}_5$ , the evaporation is more fierce than that of 1800  $^{\circ}\text{C}$ . So, flat steps can be found, which did not appear in the surface temperature curve at 1800  $^{\circ}\text{C}$ .

From the macro images (Fig. 3b–e) of the ablated samples, great differences happen to the samples' surface. At 2100  $^{\circ}\text{C}$ , deep pits exist in the central region; the coating has been broken through after ablation for 60 s; the black matrix can be seen in the image. At 1900  $^{\circ}\text{C}$ , fusant appeared in border region, but the coating is still integrated in centre region. At 1800  $^{\circ}\text{C}$ , most fusant assembled in centre region and no fusant was blown to the border region.

At 2100  $^{\circ}\text{C}$ , the temperature is much higher than the melting point of  $\text{Ta}_2\text{O}_5$ . The fusant had higher liquidity and lower viscosity, The coherence between the fusant and coating became very poor. Most fusant was blown away by the flame and little remained on the surface. The fusant would not behave positive ability to the ablation resistance. Therefore, the composites were attacked severely by the flame, deep pits can be found in centre region. The coated composites have bad ablation resistance and showed high ablation rates ( $1.2 \times 10^{-2} \text{ mm/s}$  and  $3.9 \times 10^{-3} \text{ g/s}$ , Fig. 4) at this temperature. However, the fusant had a higher viscosity and lower liquidity at 1900 and 1800  $^{\circ}\text{C}$ . They can adhere to the inner coating and

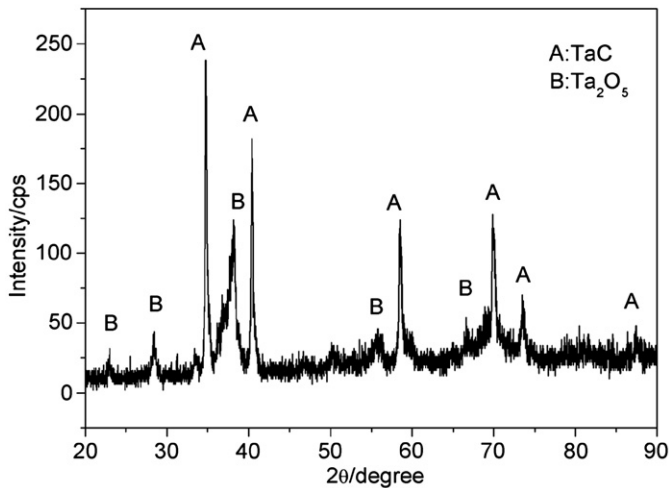


Fig. 1. XRD patterns of as-received TaC/SiC coating.

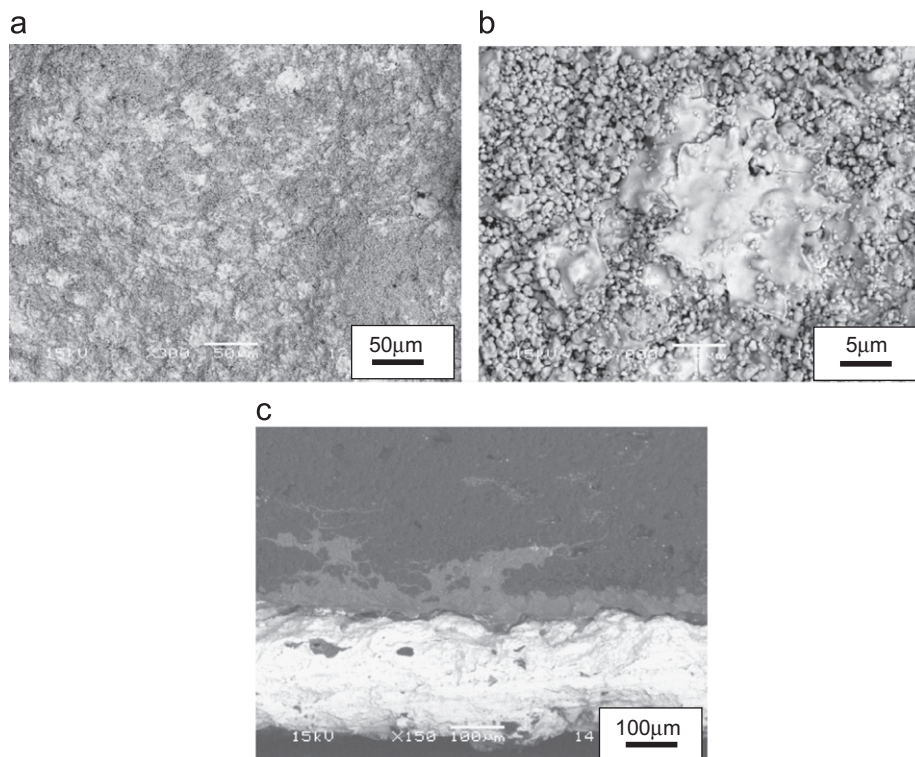


Fig. 2. Surface and cross section SEM images of TaC/SiC coating.

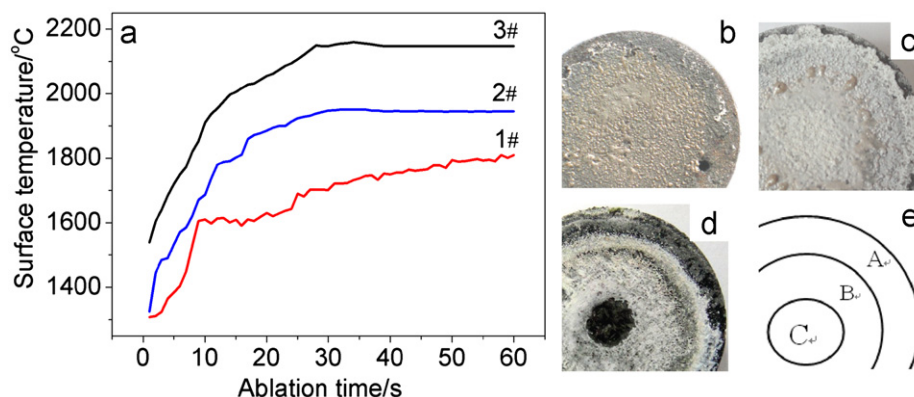


Fig. 3. The surface temperature and the macro images of the coated samples at different temperature. (a) (1#:1800 °C, 2#:1900 °C, 3#:2100 °C), (b) :1# (c) :2# (d) :3# (e) (ablation region sketch. (C): centre region, (B): transition region, (A): border region).

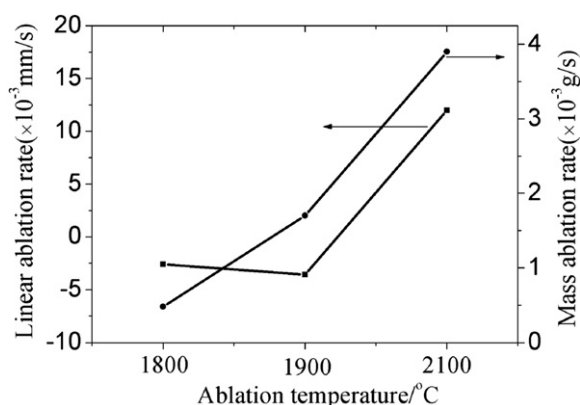


Fig. 4. The ablation properties of coated samples at different temperatures.

provide efficient protection. Both the linear ablation rates are minus ( $-3.58 \times 10^{-3}$  mm/s and  $-2.6 \times 10^{-3}$  mm/s), that is, the coating behaved zero ablation. The mass ablation rates are  $1.7 \times 10^{-3}$  g/s and  $0.48 \times 10^{-3}$  g/s, respectively, which are also much lower than that at 2100 °C. At 1800 °C, almost no fusant was blown away, therefore TaC coating behaved lowest mass ablation rate.

Fig. 5a and b are the images after 60 s ablation at 2100 °C. The fibres were burned into cone shape. Somewhere the fibres were cut off by flame shear force, only holes were left. No oxides can be found on surface. It can be inferred that the coating has failed completely. The irregular shaped pits on the matrix and fibres verified that the composites suffered severe ablation under oxyacetylene torch.

In order to research the oxides state change, the morphology in centre region for 20 s ablation is presented in Fig. 5c and d. The coating has been broken through, the matrix cannot be protected. The fusant presented not as a coating but spheres, which covered on the fibres. The fibre appeared as rough surface. Additionally, some hemispherical pits can be found on fibre surface. From the magnified photo (Fig. 5d), tiny residual Ta<sub>2</sub>O<sub>5</sub> or SiO<sub>2</sub> spheres can be found at the pit bottom. It is deduced that the oxides may accelerate the corrosion to the fibres.

During ablation, the evaporation and melt of Ta<sub>2</sub>O<sub>5</sub> and SiO<sub>2</sub> can consume a lot of heat, it is positive to the ablation protection. However, unlike the positive effect of oxides on the ablation resistance in matrix modified C/C composites [18], the oxides cannot be provided continuously. Its positive effect is very slight. The oxides were mostly inclined to accelerate the corrosion to the fibres. It is because the oxides reacted with carbon matrix according to Eqs. (5)–(8). After that, the TaC and SiC continued to react with oxygen and generate oxides again (Eqs. (3), (4), (9) and (10)). In this process, the carbon was the only consumed substance. The residual oxides just served as catalyst and did not consume according to these reactions. The acceleration would not stop until the residual oxides were blown out. The oxides were spherical at 2100 °C, they corroded the fibres so that the pits presented as hemisphere-shaped. When the big spheres were blown away, tiny ones remained in the pits bottom.

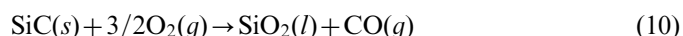
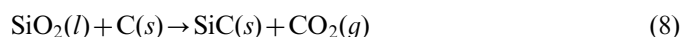
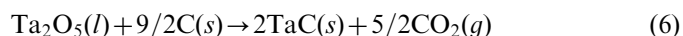
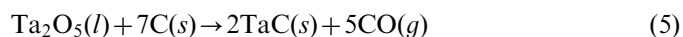


Fig. 6 shows the SEM images of centre region after ablation for 60 s at 1900 °C. Much fusant appeared on surface. However, Ta<sub>2</sub>O<sub>5</sub> can still be blown away but just to the border region at this temperature. From Fig. 6a, the ablation mechanism of the coating can be inferred. During ablation, the bulge place on surface is more close to the nozzle tip and has higher temperature than the other places. So, Ta<sub>2</sub>O<sub>5</sub> melted firstly there. Because of mechanical denudation of the flame, partial Ta<sub>2</sub>O<sub>5</sub> was blown away. Then, an ablation pit formed there, which is presented in the centre of Fig. 6a. However, the pits edge became into bulge place, and underwent the same process, as ablation going. The circulation repeated until the



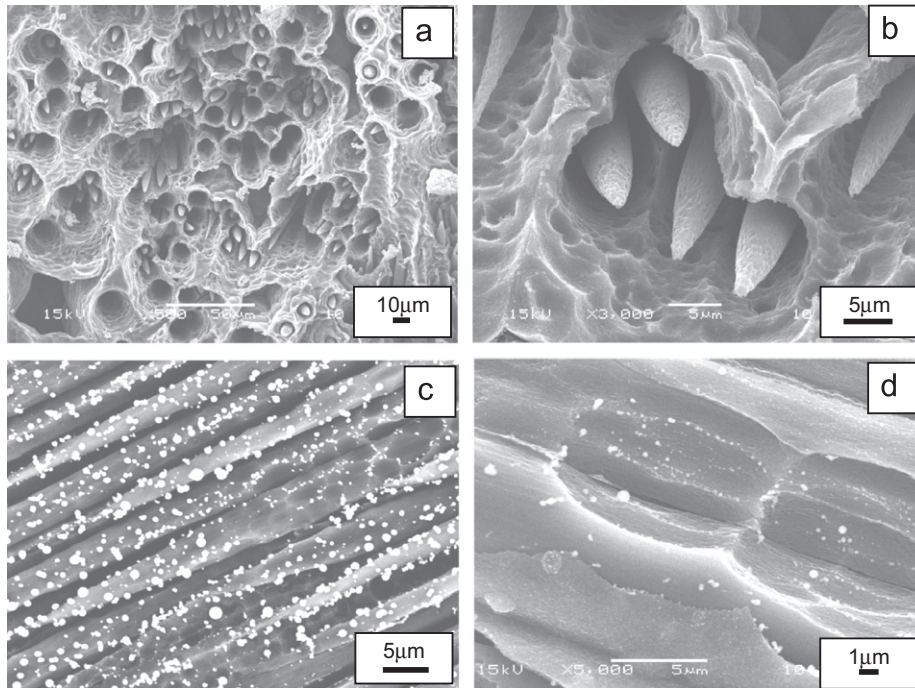


Fig. 5. SEM image of ablation centre region at 2100 °C (a and b) 60 s, (c and d) 20 s.

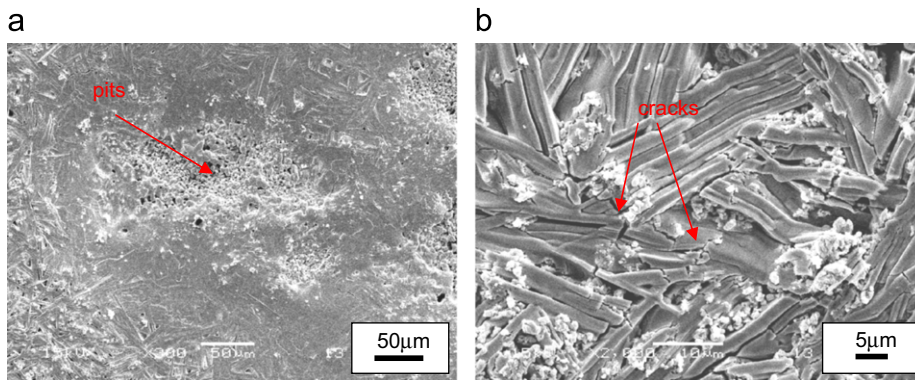


Fig. 6. SEM images of centre region at 1900 °C.

coating was broken through. According to the ablation rates at 1900 °C, the coating exhibited good ablation resistance. It can be concluded that the mechanical denudation did damages to the coating, but it could not ruin the integrality of the coating and affect the ablation resistance. From Fig. 6b, it can be seen that the fusant existed as dendrites after ablation. It is because that the fusant is composed of monoclinic  $\text{Ta}_2\text{O}_5$  (Fig. 7). The phase has a high viscosity and is apt to form branch-like crystalline, when cooled down from high temperature. The dendrites have large size. Cracks can be found on the surface, which may provide channels for oxygen and result in oxidation of inner coating or composites.

However, the surface is much different at 1800 °C (Fig. 8). The surface is flat, some micro holes can be found and the fusant distributes uniformly in centre region (Fig. 8a). The size of branch-like crystalline is much smaller than that at 1900 °C, and no obvious cracks are

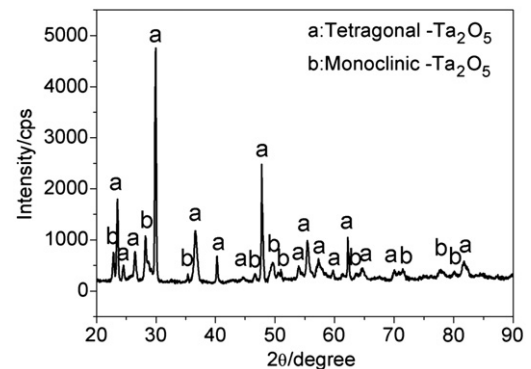


Fig. 7. The XRD pattern of centre region after ablation.

found on the surface (Fig. 8b). The melting  $\text{Ta}_2\text{O}_5$  formed a dense coating on the surface. It is advantageous for the ablation resistance. The melting coating can serve as a

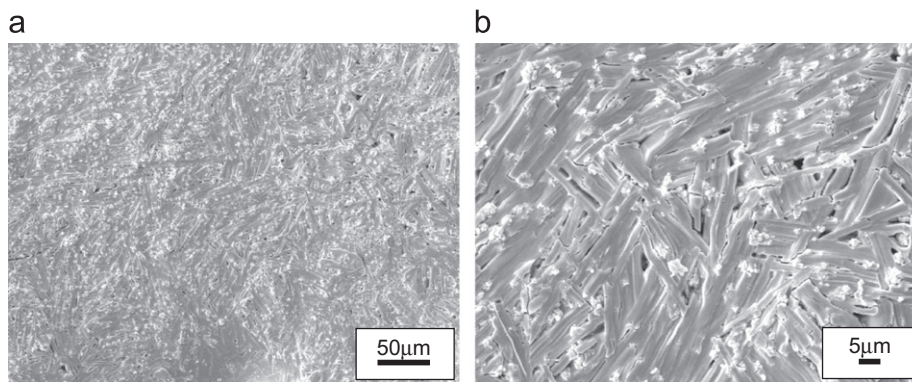


Fig. 8. SEM images of centre region at 1800 °C.

thermal barrier layer and bring down the inner temperature of the coating. Meanwhile, the melting  $\text{Ta}_2\text{O}_5$  had a low oxygen-diffusing coefficient and prevented inner coating from oxidation. Therefore, the coating exhibited better ablation resistance at this temperature.

It can be concluded that the state of oxides during ablation is very important for ablation resistance properties of the TaC coating on SiC coated C/C composites. When the temperature is just below the oxide melting point, the oxide fusant has a proper viscosity to form a glassy coating on the surface. The glassy coating can provide a thermal and oxygen diffusing barrier for the inner coating. The mechanical denudation and the oxidation mechanism can be held furthest. If the temperature is much higher than oxide melting point, the viscosity is so low and the melting oxides can be blown away through mechanical denudation. The coating will be broken through rapidly.

#### 4. Conclusions

A TaC/SiC coating was prepared through diffusing reaction and supersonic plasma spraying method. Surface temperature stayed at a fixed value after 30 s ablation under oxyacetylene torch, owing to the oxides evaporation. The TaC/SiC coating showed better ablation resistance at 1900 and 1800 °C. The oxides can remain in ablation centre because of their high viscosity. The oxides served as coating during ablation and provided efficient protection for composites. At 2100 °C, the viscosity of oxides was so low that the melts were blown away by the flame. Moreover, the residual oxides accelerated the corrosion to C/C composites after the coating was broken through.

#### Acknowledgements

This work has been supported by the National Natural Science Foundation of China under Grant Nos. 51072166 and 50902111, the Program for New Century Excellent Talents in University, the Research Fund of State Key Laboratory of Solidification Processing (NWPU), China

(Grant No. 25-TZ-2009) and “111” Project (Grant No. B08040).

#### References

- [1] J.D. Buckley, D.D. Edie, Carbon—Carbon Materials and Composites, Noyes Publication, 1993 (pp. 267–279).
- [2] C.R. Thomas, Essential of carbon-carbon composites, The Royal Society of Chemistry (1993) 26–33.
- [3] H.J. Li, Carbon/carbon composites, New Carbon Materials 16 (2001) 79–80.
- [4] C.P. Leonard, R.M. Amundsen, W.E. Bruce, Hyper X hot structures design and comparison with flight data, in: Proceedings of the 13th AIAA/CIRA International Space Planes and Hypersonic Systems and Technologies Conference, Capua, Italy, AIAA, 2005.
- [5] J.J. Choury, Carbon-carbon materials for nozzles of solid propellant rocket motors, in: Proceedings of the 12th Propulsion Conference, Palo Alto, CA, AIAA, 1976.
- [6] N. Ahlen, M. Johnsson, M. Nygren, Oxidation behaviour of  $\text{Ta}_x\text{Ti}_{1-x}\text{C}$  and  $\text{Ta}_x\text{Ti}_{1-x}\text{C}_y\text{N}_{1-y}$  whiskers, Thermochemica Acta 336 (1999) 111–120.
- [7] Y.J. Chen, J.B. Li, H.Z. Zhai, Preparation and growth mechanism of  $\text{TaC}_x$  whiskers, Journal of Crystal Growth 224 (2001) 244–250.
- [8] H. Xiang, Y.D. Xu, L.T. Zhang, L.F. Cheng, Synthesis and microstructure of tantalum carbide and carbon composite by liquid precursor route, Scripta Materialia 55 (2006) 339–342.
- [9] Y. Wang, Y.D. Xu, L.T. Zhang, L.F. Cheng, Ablation resistance properties and mechanism of 3D C/SiC-TaC composites, Aerospace Materials and Technology 3 (2009) 41–44.
- [10] Z.K. Chen, X. Xiong, G.D. Li, Y.L. Wang, Ablation behaviours of carbon/carbon composites with C-SiC-TaC multi-interlayers, Applied Surface Science 255 (2009) 9217–9223.
- [11] Z.J. Dong, X.K. Li, G.M. Yuan, Y. Cong, N. Li., Z.J. Hu, Z.Y. Jiang, A. Westwood, Fabrication of protective tantalum carbide coatings on carbon fibers using a molten salt method, Applied Surface Science 254 (2008) 5936–5940.
- [12] H.W. He, C.K. Zhou, X. Xiong, Preparation of TaC ablation resistance coating on C/C composites, Rare Metal Materials and Engineering 33 (2004) 490–493.
- [13] G.D. Li, X. Xiong, B.Y. Huang, K.L. Huang, Structural characteristics and formation mechanisms of crack-free multilayer TaC/SiC coatings on carbon-carbon composites, Transactions of Nonferrous Metals Society of China 18 (2008) 255–261.
- [14] Z.K. Chen, X. Xiong, G.D. Li, W. Sun, Y. Long, Texture structure and ablation behaviour of TaC coating on carbon/carbon composites, Applied Surface Science 257 (2010) 656–661.
- [15] H. Wu, H.J. Li, Q.G. Fu, D.J. Yao, Y.J. Wang, Chao Ma, Microstructures and ablation resistance of ZrC coating for SiC-coated

- carbon/carbon composites prepared by supersonic plasma spraying, *Journal of Thermal Spray Technology* 20 (2011) 1286–1291.
- [16] Z.H. Han, B.S. Xu, H.J. Wang, S.K. Zhou, A comparison of thermal shock behaviour between currently plasma spray and supersonic plasma spray  $\text{CeO}_2\text{--Y}_2\text{O}_3\text{--ZrO}_2$  graded thermal barrier coatings, *Surface and Coating Technology* 201 (2007) 5253–5256.
- [17] K.Z. Li, D.S. Hou, H.J. Li, Q.G. Fu, G.S. Jiao, Si–W–Mo coating for SiC coated carbon/carbon composites against oxidation, *Surface and Coating Technology* 201 (2007) 9598–9602.
- [18] X.T. Shen, K.Z. Li, H.J. Li, H.Y. Du, W.F. Cao, F.T. Lan, Microstructure and ablation properties of zirconium carbide doped carbon/carbon composites, *Carbon* 48 (2010) 344–351.